Electronic Supplementary Material (ESI) for Journal of Materials Chemistry A.

Supplementary Information for:

Engineering Hollow Back Electrode for Hybrid Solar Cells towards Efficient Light Harvesting and Carrier Collection

Peng-Fei Yin,[a] Jing-Jing Wang,[a] Yu-Zhu Zhou, [a] Jing Mao, [a] Wen-Jing Qin,[b] Shi-Zhang Qiao,[a,c] Tao Ling [a] and Xi-Wen Du [a]**

[a] Institute of New-Energy Materials, Key Laboratory of Advanced Ceramics and Machining Technology, Ministry of Education, School of Materials Science and Engineering, Tianjin University, Tianjin, 300072, China

[b] Institute of Material Physics, Tianjin University of Technology,Tianjin 300384, China

[c] School of Chemical Engineering , The University of Adelaide ,Adelaide, SA 5005, Australia

* Correspondence and requests for materials should be addressed to T. L and X.-W.D. (email: lingt04@tju.edu.cn and xwdu@tju.edu.cn).

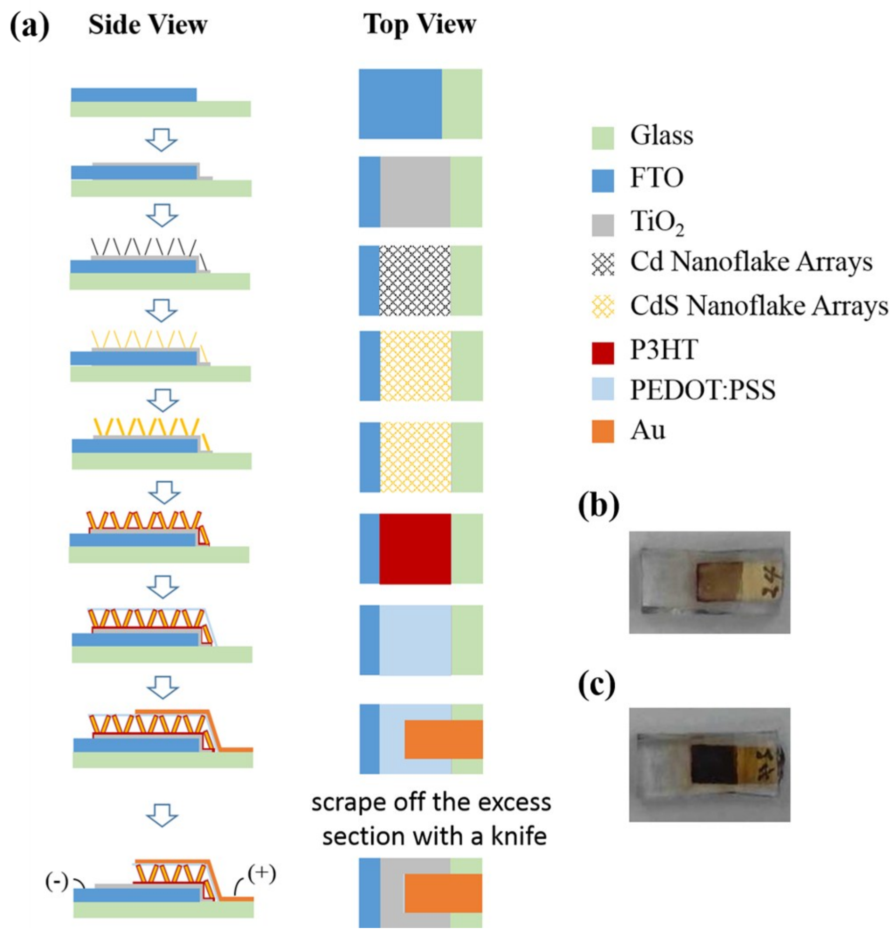

Fig. S1. (a) Schematic preparation process of the CdS/P3HT H-HSC. (b, c) Photographs of the CdS/P3HT H-HSC from (b) top-side and (c) back-side.

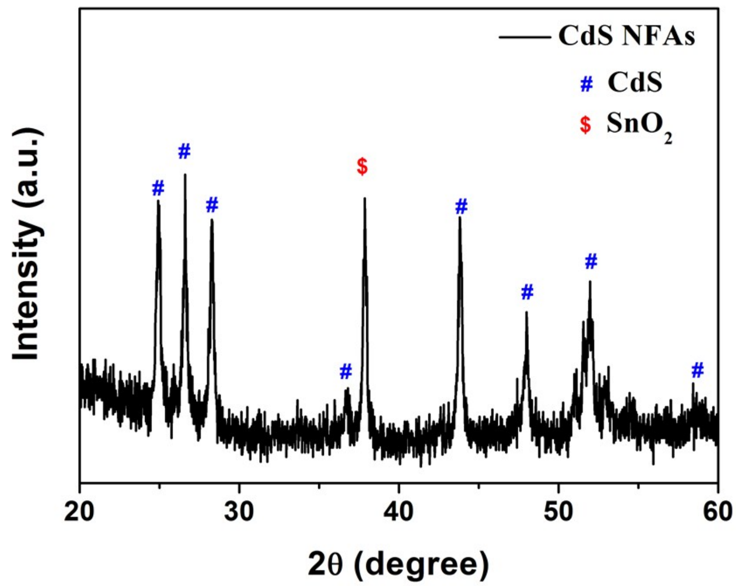

Fig. S2. XRD pattern of the CdS NFAs deposited onto FTO glass.

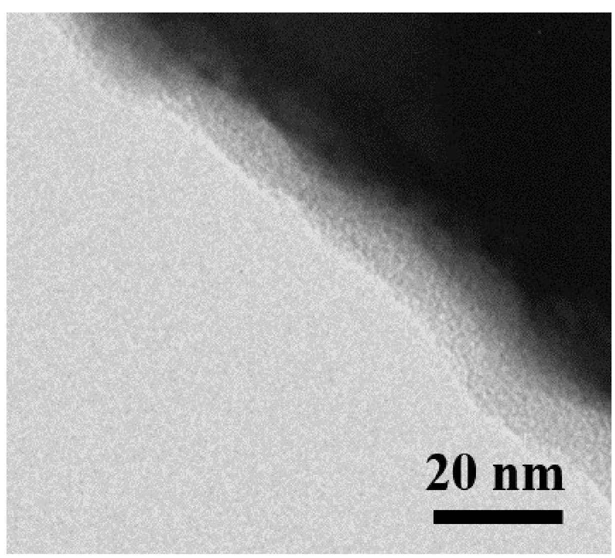

Fig. S3. TEM image of the CdS nanoflake coated with P3HT.

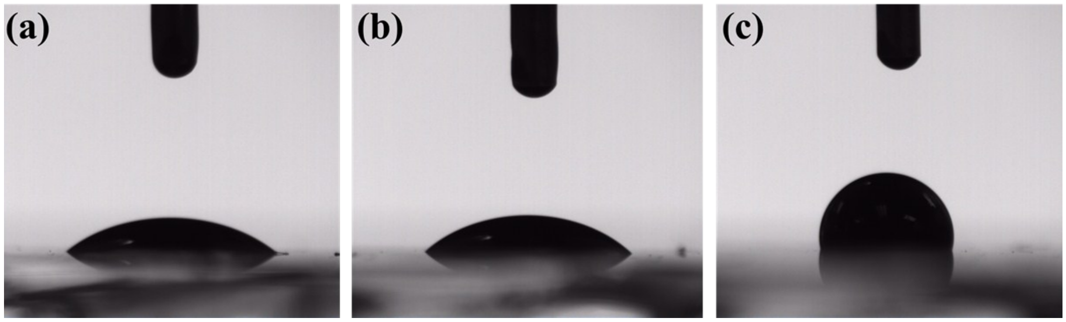

Fig. S4. The wetting angles of (a) PEDOT:PSS solution diluted with two volumes of isopropanol with a value of 37°, (b) PEDOT:PSS solution diluted with one volume of isopropanol with a value of 40.5° and (c) PEDOT：PSS aqueous solution without isopropanol with a value of 99°. The substrate is a slice of FTO with P3HT coating.

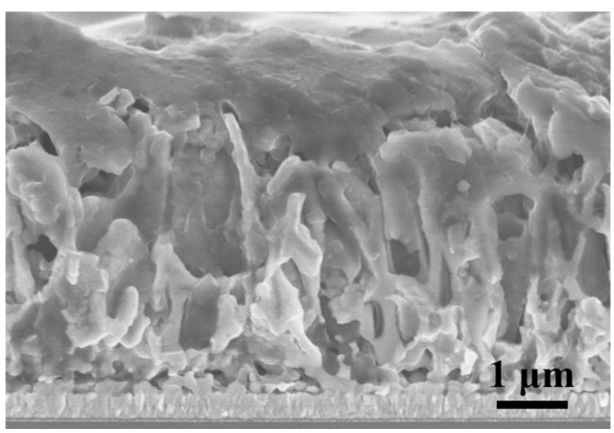

Fig. S5. Side-view SEM image of the CdS NFAs with fully-infiltrated P3HT (S-HSC).

The optimization of the thickness of Au layer in CS-HSC.

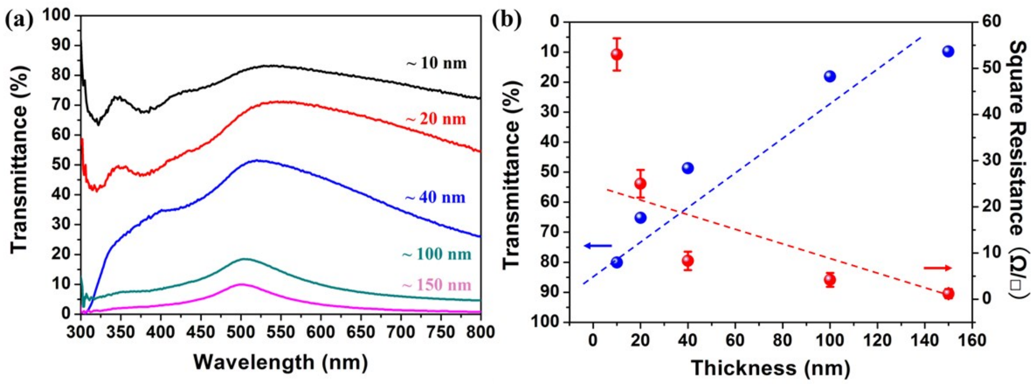

Fig. S6. (a) Transmittance spectra of the Au films deposited onto the glass with different thickness. (b) The chats of transmittance (left coordinate) and square resistance (right coordinate) of Au layer which was deposited on the glass slide by sputtering method as the function of film thickness.

According to Fig. S6b, both the transmittance and square resistance of the Au layer decrease with the increasing film thickness. As being a counter electrode, in order to meet both the requirements of the high transparent and conductive, the thickness of the Au film used in our experiment was selected as ~30 nm (Fig. S6b).

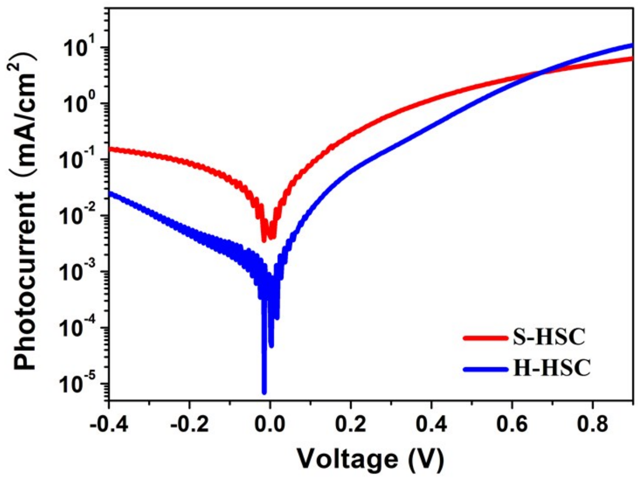

Fig. S7. J-V curves of the S-HSC and H-HSC measured in dark.

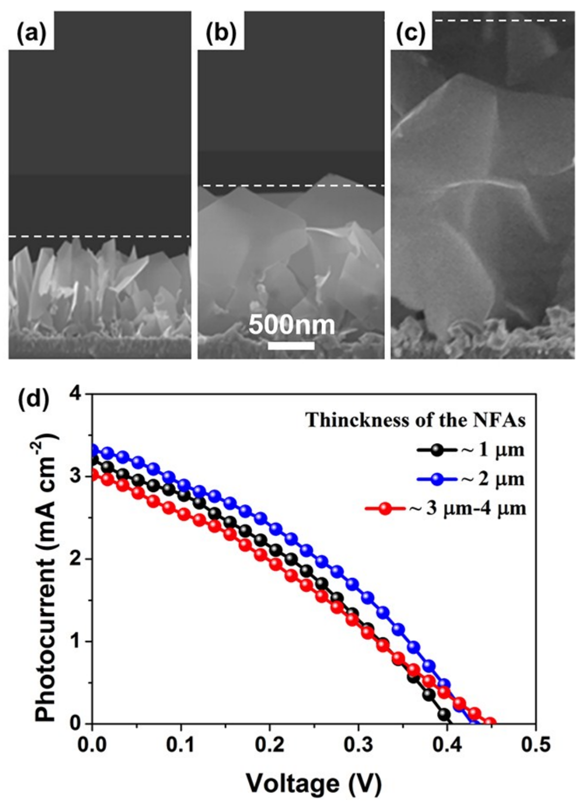

Fig. S8 SEM images of Cd NFAs with flake size of (a) 1 μm, (b) 2 μm, (c) 3-4 μm. By furthe sulfurization, Cd NFAs can be transformed into CdS NFAs with the maintained morphology and thickness. (d) The J-V curves of the HSCs with different NFAs thicknesses.

Table S1. J-V characteristics of CdS/ P3HT H-HSCs with different array thickness.

NFAs thickness	J_{sc} [mA cm^{-2}]	V_{oc} [V]	η [%]
~1 μm	3.2	0.4	0.45
~ 2 μm	3.4	0.43	0.52
~ 3 -4 μm	3.04	0.45	0.41

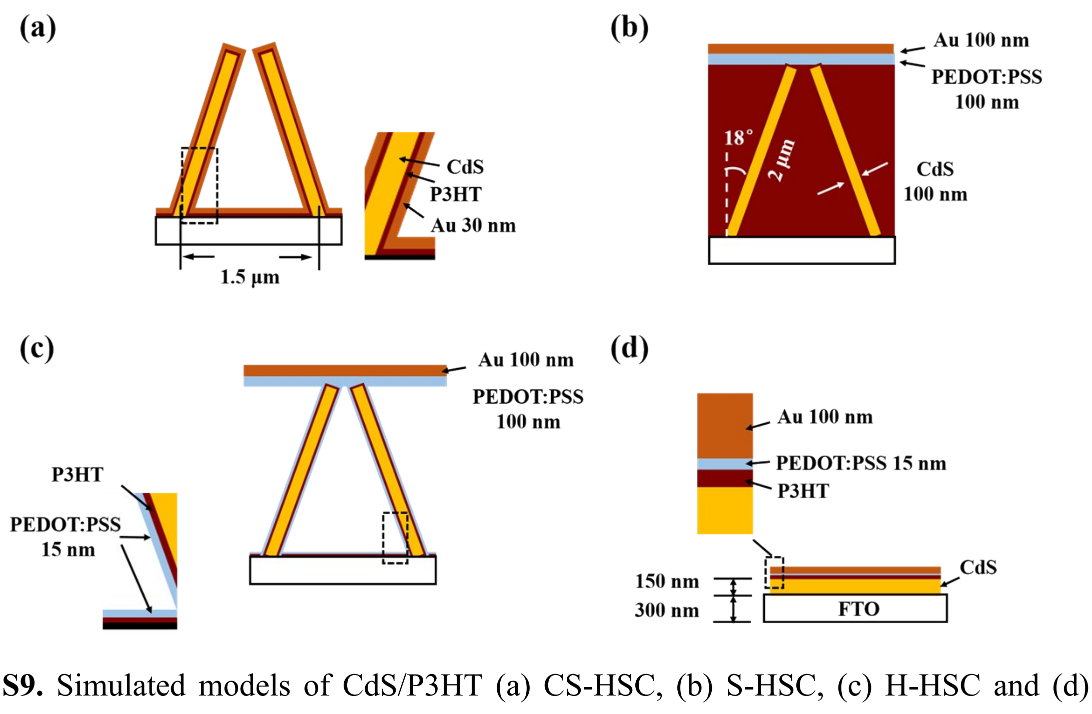

Fig. S9. Simulated models of CdS/P3HT (a) CS-HSC, (b) S-HSC, (c) H-HSC and (d) bilayer planar HSC.

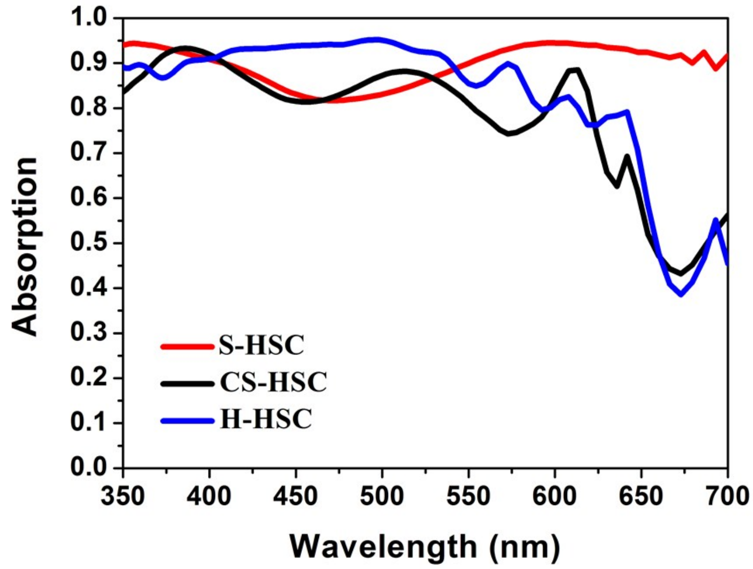

Fig. S10. Calculated absorption spectra of S-HSC, CS-HSC and H-HSC.

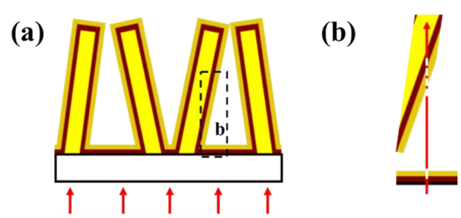

Fig. S11. Diagram of the light path when incident light comes from the FTO side.

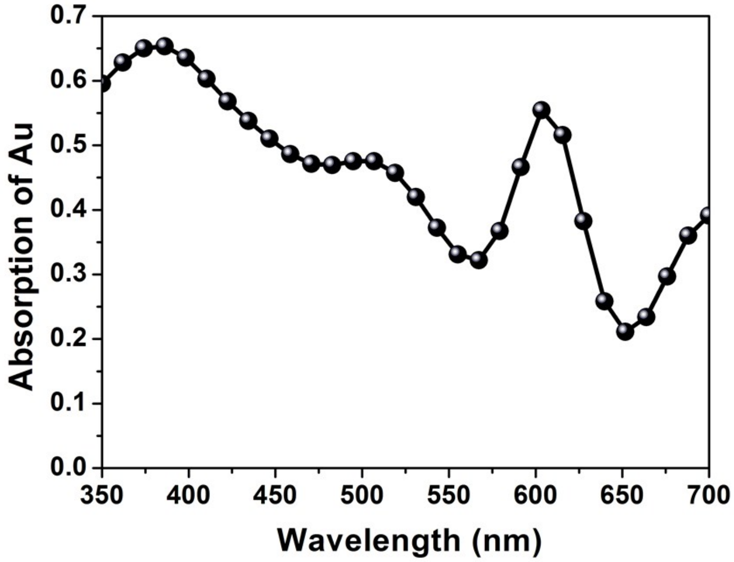

Fig. S12. Calculated absorption spectrum of Au in CS-HSC.

The characterizations of CdS/P3HT planar bilayer HSC.

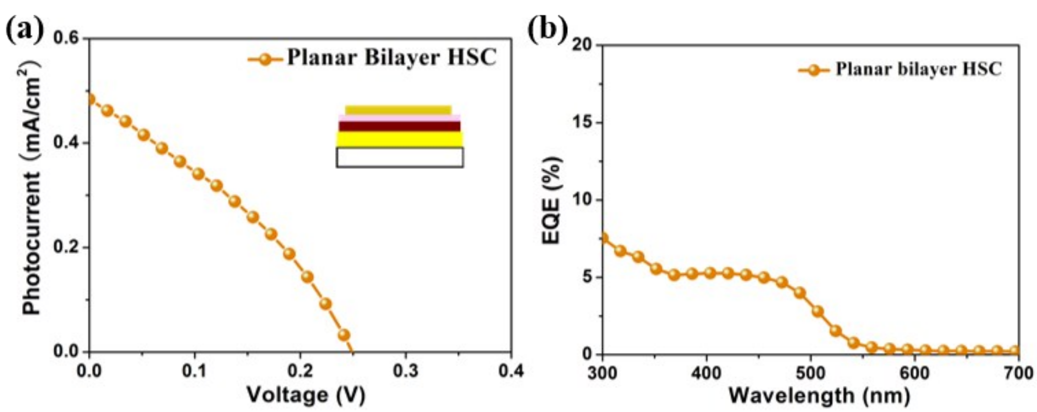

Fig. S13. Photovoltaic properties of the planar bilayer HSC. (a) J-V curve, and the inset is a schematic map of CdS/P3HT planar bilayer HSC. (b) IPCE spectrum.

Table S2. J-V characteristics for planar bilayer HSCs.

device	J_{sc} [mA cm^{-2}]	V_{oc} [V]	FF [%]	η [%]
Planar bilayer HSC	0.48	0.25	33	0.04

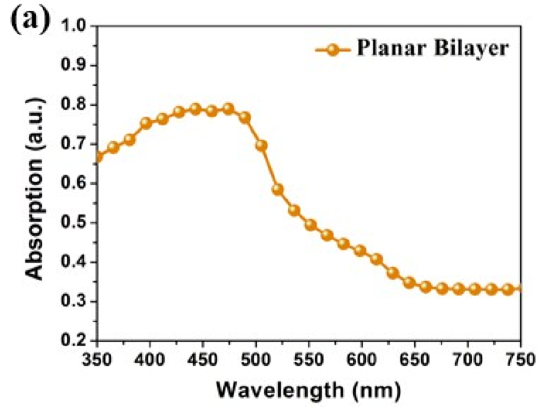

Fig. S14. Optical measurements of the planar bilayer HSC. (a) Absorption spectra. (b) Simulated absorption profiles of the CdS/P3HT planar bilayer HSC under 500 nm illumination.

EIS measurements.

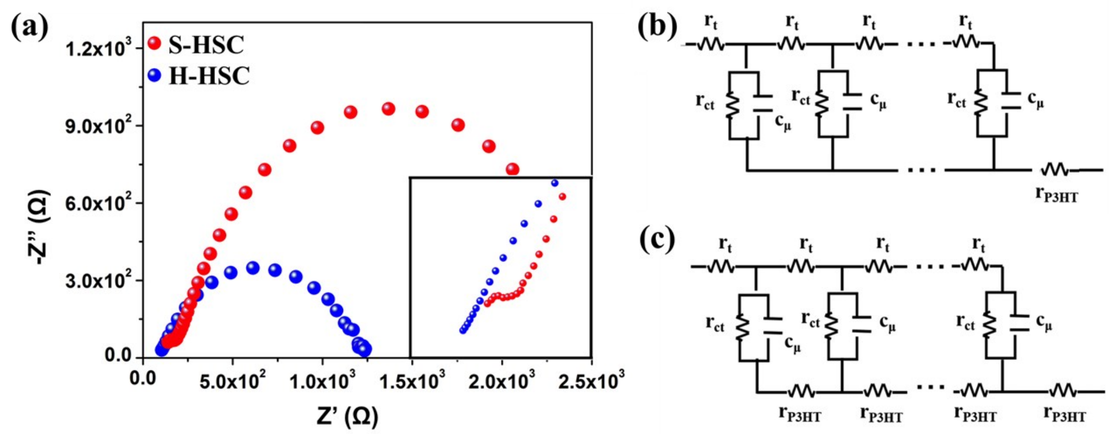

Fig. S15. (a) Nyquist plots of H-HSC and S-HSC measured under 1 sun illumination. The inset image is the enlarged Nyquist plots of (a) at high frequencies. (b) Transmission line model used to fit the impedance data. (c) Two-channel resistance transmission line model used to fit the impedance data.

Fig. S15a presents the Nyquist plots of H-HSC and S-HSC measured under 1 sun illumination at 0 V applied bias. The H-HSC follows well a transmission line model, as shown in Fig. S15b.[1] Meanwhile, the additional arc appears in the S-HSC (Fig. S15a inset) which arises from the complex behavior of the infiltrated P3HT. Hence, two-channel resistance transmission line model (Fig. S15c) was adopted to fit the impedance data of S-HSC.[1]

The calculation of the electron mobility in CdS NFAs.

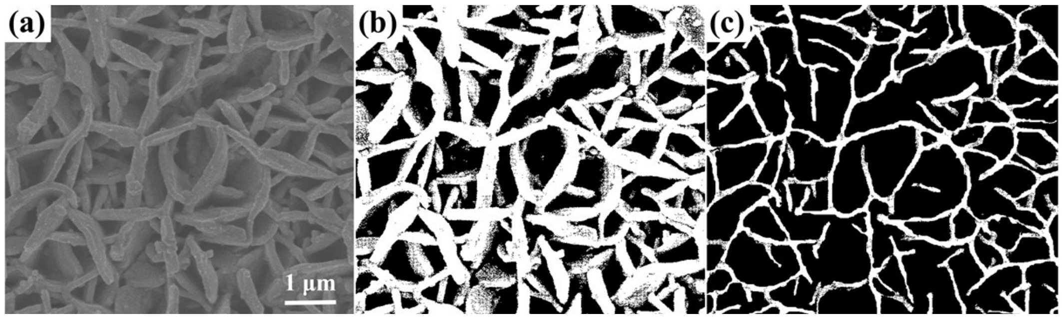

Fig. S16. (a) Original top-view SEM image of the CdS NFAs. (b) Corresponding SEM image after color contrast. (c) Corresponding image after further manual adjustment. The active area fraction of CdS NFAs can be calculated with a value of 20.3 %.

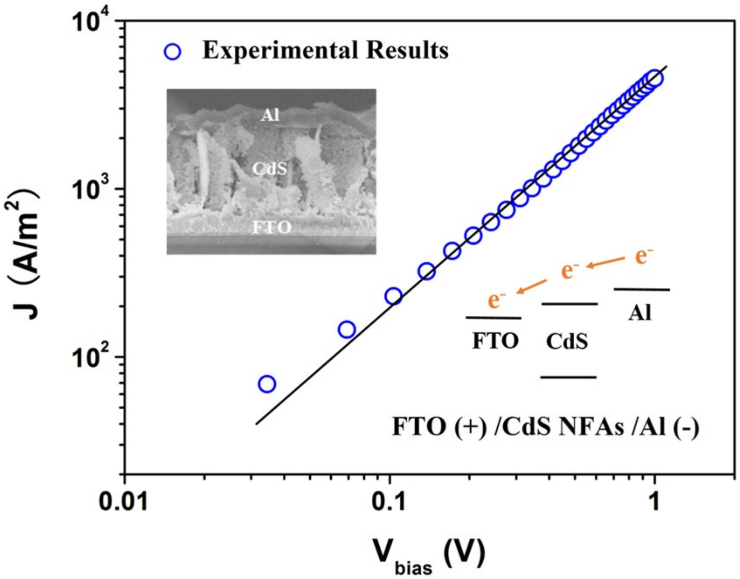

Fig. S17. Experimental (open circle symbols) and fitting (solid line) J-V curves of the FTO/CdS NFAs/Al device measured in dark. Side-view SEM image and band diagram of the device are shown in the inset. Notably, the current density used here is given by,

$J = I/(S_{nominal} \times 20.3\ \%)$, where I represents measured current and $S_{nominal}$ represents the nominal area of the device.

To measure the electronic mobility in the CdS NFAs, the active area fraction of the CdS flakes was first calculated from the typical top-view SEM image with a value of 20.3 % (Fig. S16). Then an additional electron dominated device was assembled by sandwiching the CdS NFAs between FTO and Al (see the inset in Fig. S17). As depicted in Fig. S17, the electrical current depends quadratically on V_{bias}, which suggests that the charge transfer in CdS follows the space-charge limited conduction law,[2-4]

$$J = \frac{9}{8}\varepsilon_0 \varepsilon_r \mu \frac{V^2}{L^3} \tag{1}$$

Where J is the current density, which is approximately given by $J = I/(S_{nominal} \times 20.3\ \%)$, I represents measured current and $S_{nominal}$ represents the nominal area of the device, μ is the electron mobility, V is the applied voltage, ε_0 is the permittivity (8.85×10^{-14}, F cm^{-1}), ε_r is the relative permittivity of the material, for CdS is 11.6, and L is the thiSckness of photoactive layer (~2 μm). By fitting the curve with equation (1), the mobility of CdS NFAs can be worked out with the value of 1.59 $cm^2V^{-1}S^{-1}$, agreeing well with the reported CdS film.[5]

The characterizations of CdSe/P3HT HSC.

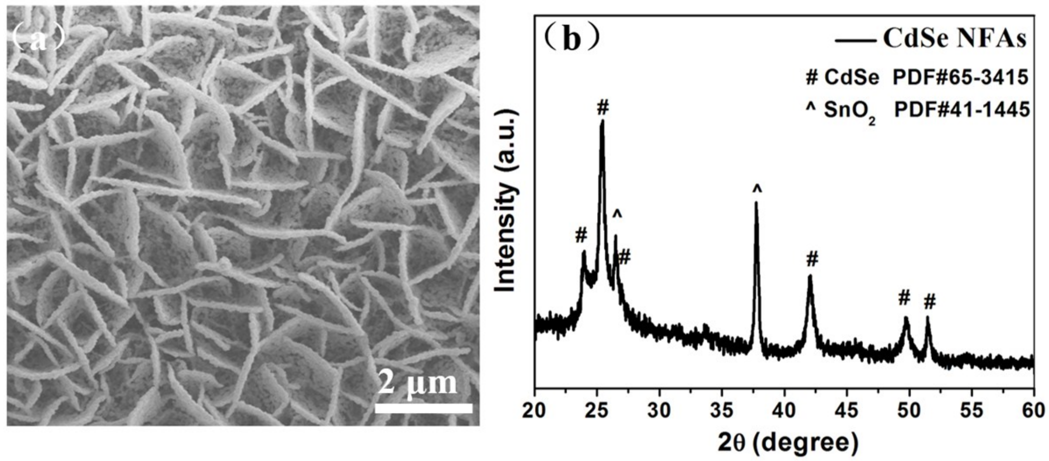

Fig. S18. Characterizations of the CdSe NFAs. (a) Top-view SEM image, and (b) XRD pattern.

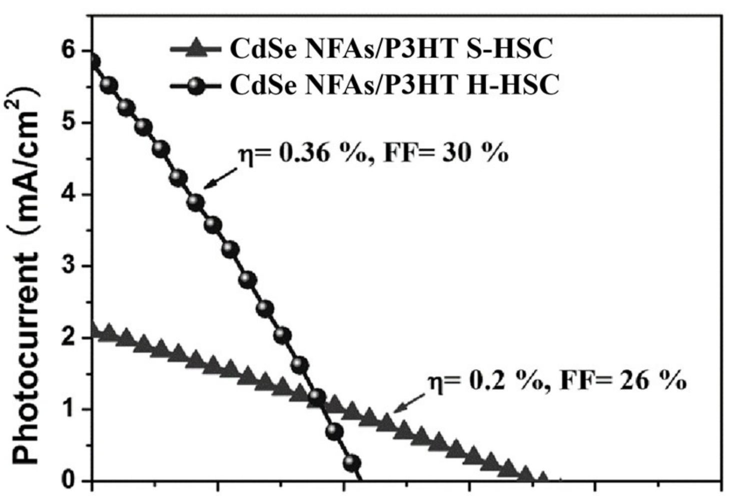

Fig. S19. J-V curves of CdSe NFAs/P3HT S-HSC and CdSe NFAs/P3HT H-HSC.

Table S3. J-V characteristics of CdSe network/P3HT HSCs.

device	J_{sc} [mA cm^{-2}]	V_{oc} [V]	η [%]	References
CdSe NFAs/P3HT H-HSC	5.8	0.21	0.36	This work
CdSe NFAs/P3HT S-HSC	2.1	0.36	0.2	This work
CdSe nanorode array/P3HT HSCs	4.79±0.72	0.49±0.02	1±0.14	6

References

1 F. Fabregat-Santiago, J. Bisquert, L. Cevey, P. Chen, M.K. Wang, S.M. Zakeeruddin, M. Gratzel, *J. Am. Chem. Soc.*, **2009**, 131, 558-562.

2 Y.X. Nan, F. Chen, L.G. Yang, H.Z. Chen, *J. Phys. Chem. C*, **2010**, 114, 11911-11917.

3 V.D. Mihailetchi, J.K. J. van Duren, P.W.M. Blom, J.C. Hummelen, R.A.J. Janssen, J.M. Kroon, M.T. Rispens, W.J.H. Verhees, M.M. Wienk, *Adv. Funct. Mater.*, **2003**, 13, 43-46.

4 P.W.M. Blom, M.J.M. de Jong, J.J.M. Vleggaar, *Appl. Phys. Lett.*, **1996**, 68, 3308-3310.

5 K.R. Murali, K. Thilakawathy, S. Vasantha, R. Oomen, *Chalcogenide Lett.*, **2008**, 5, 164-169.

6 M. Schierhorn, S.W. Boettcher, J.H. Peet, E. Matioli, G.C. Bazan, G.D. Stucky, M. Moskovits, *ACS nano*, **2010**, 4, 6132-6136.